



How the Oblate Spheroidal Coordinates Facilitate Modeling of Quantum Rings

V. A. Roudnev^{1,a}, A. M. Puchkov¹ and A. V. Kozhedub¹

¹ Physics Department, St. Petersburg State University, Universitetskaya nab. 7-9, St. Petersburg, 199034 Russia

e-mail: ^a v.rudnev@spbu.ru

Received 28 February 2017, in final form 15 March 2017. Published 21 March 2017.

Abstract. We propose a new approach for modeling three-dimensional single particle quantum rings based on separation of variables in oblate spheroidal coordinates. This approach has an advantage in the variety of the ring cross sections that can be modeled with high computational efficiency. We illustrate this by studying the shape dependence of the energy spectrum for a single particle confined to the ring of triangular cross section. The spectrum can demonstrate parabolic or non-parabolic behavior as a function of the magnetic quantum number depending on the ring profile.

Keywords: quantum rings, spectrum, shape

PACS numbers: 73.21.-b, 73.22.Dj, 71.15.-m

1. Introduction

Quantum dots and quantum rings are becoming irreplaceable components of modern electronics due to the arising technological opportunity to control their spectral properties accurately. Such structures as multiple concentric nano-rings, rings around a quantum dot and many other complex nano-objects are been fabricated on the base of droplet epitaxy [1, 2, 3]. Fabrication methods for creating regular two- and three-dimensional structures of nano-rings are also being developed on the base of nanospherical lithography [4, 5, 6].

Despite an obvious progress in fabricating nano-objects, however, an efficient theoretical and computational description is still a challenging problem. Even for single-particle states, we have an alternative: either to restrict ourselves to simplified models [7, 8, 9], or to resort to computationally costly calculations for taking into account the three-dimensional structure of the systems [10, 11]. In this work we suggest an approach which on the one hand allows us to treat quite complex three-dimensional ring-shaped nano-structures, and on the other hand to reduce the computational cost of the model by exact separation of variables in oblate spheroidal coordinates.

It is well known, that the two types of the spheroidal coordinates – prolate and oblate – both admit separation of variables for the Schrödinger equation [12, 13]. Even though there are only a few known quantum problems with exact separation of variables, it is the prolate spheroidal coordinates that are preferably used in hundreds of published researches. The oblate spheroidal coordinates, however, have been used rather rarely in quantum mechanical calculations. There are only a few such papers known to the authors. The most famous example is, probably, the work of Rainwater [14], where the model of a spheroidal infinitely deep potential well made it possible to explain magnetic moments of many nuclei based on the behavior of an unpaired nucleon. Another example of using oblate spheroidal coordinates is given in [15], where the optical properties of spheroidal quantum dots are discussed.

In this article we demonstrate how the use of oblate spheroidal coordinates allowed us to make some curious observations on the variations of quantum ring spectra as the ring shape changes.

Even though separation of variables in cylindrical coordinates – which are being used routinely in quantum ring calculations – also gives a computationally efficient scheme, it also has an important limitation: only rectangular cross sections can be reproduced efficiently. The flexibility of oblate spheroidal coordinate system is such that it makes possible to model not only the rings of rectangular cross section, but also the more realistic triangular – and even more complex – cross sections as well [16, 17]. Here we put our special attention to the rings of triangular cross section.

It is worth mentioning that J. Even and S. Loualiche [18] have also considered a model of a quantum ring bounded by an infinite potential wall. In their case, the boundary of the ring is formed by circular paraboloides and the separation of variables is performed in parabolic coordinates. The advantage of our approach is that it allows us to vary the shape of the ring while fixing its volume and the

characteristic size R , which, basically, has made our study possible. In our approach it is also possible to model a flat substrate directly without solving an auxiliary problem for a symmetric ring and post-selecting the solutions that fit the required boundary condition.

The major goal of this work is to demonstrate suitability of oblate spheroidal coordinates for describing three-dimensional nano-scale quantum rings. For this purpose we use a simple model of a particle confined to a ring-like structure by an infinite potential wall. This approach not only allowed us to develop a computationally simple scheme for ring spectrum calculations, but also to study the dependence of such spectra on the shape of the ring.

2. Quantum ring in oblate spheroidal coordinates

We employ a very simplified model of a single particle in a quantum ring. Assuming a very sharp transition between inner and outer regions of the quantum well we can neglect the effective mass inhomogeneity. As we are interested in qualitative properties of the particle confined in a ring, we use natural units (n.u.) of energy such that the Schrödinger equation for a free particle takes the following form

$$\frac{1}{2}\Delta\Psi + E\Psi = 0. \quad (1)$$

We introduce oblate spheroidal coordinates (ξ, η, φ)

$$\begin{aligned} x &= \frac{R}{2}\sqrt{(\xi^2 + 1)(1 - \eta^2)} \cos \varphi, \\ y &= \frac{R}{2}\sqrt{(\xi^2 + 1)(1 - \eta^2)} \sin \varphi, \\ z &= \frac{R}{2}\xi\eta, \\ \xi &\in [0, \infty), \quad \eta \in [-1, 1], \quad \varphi \in [0, 2\pi). \end{aligned} \quad (2)$$

We shall require the quantum well to be bounded by the coordinate surfaces $\xi = \xi_0$, $\eta = \eta_0$ and the plane $\xi = 0$, $\eta = 0$ which corresponds to a flat substrate. In Figure 1 we show a cross section of the coordinate surfaces, and the corresponding three-dimensional configuration of the ring is shown in Figure 2. Other – even more complex – combinations of coordinate surfaces can also be employed. By putting zero boundary conditions at the surface of the ring (Figure 2) we confine the particle inside the ring. Given this boundary conditions the wave function Ψ_j corresponding to the energy E_j can be represented as a product

$$\Psi_j(\xi, \eta, \varphi; R) = N_{kqm}(R) X_{mk}(\xi; R) Y_{mq}(\eta; R) e^{im\varphi}, \quad (3)$$

where the multi-index $j = \{kqm\}$ stands for a set of quantum numbers k , q and m such that k and q give the number of roots of the corresponding functions in ξ and η , while the magnetic quantum number m takes the values of $0, \pm 1, \pm 2, \dots$. The normalization constant $N_{kqm}(R)$ can be determined from the condition

$$\int_V \Psi_{kqm}^*(\xi, \eta, \varphi; R) \Psi_{k'q'm'}(\xi, \eta, \varphi; R) dV = \delta_{kk'} \delta_{qq'} \delta_{mm'}, \quad (4)$$

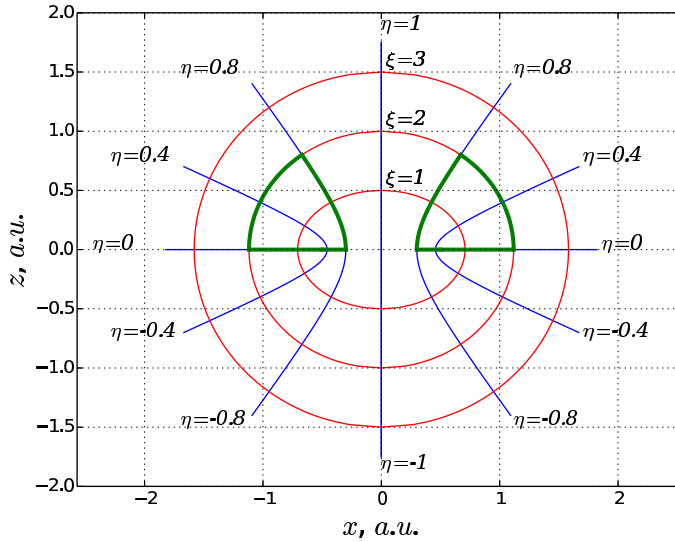


Figure 1: Oblate spheroidal coordinate surfaces projection to (x, z) -plane with z as the symmetry axis. The bold contour corresponds to a cross section of the quantum ring boundary. The three-dimensional shape of the ring is given by rotating around the z axis by the angle $0 \leq \varphi \leq 2\pi$. (Color online).

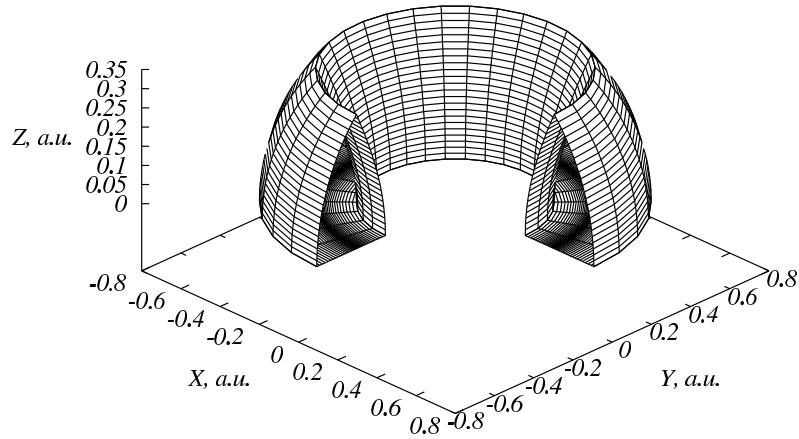


Figure 2: Isometric projection of a quantum ring, a rectangular segment is taken off to demonstrate the cross section.

where $dV = \frac{R^3}{8} (\xi^2 + \eta^2) d\xi d\eta d\varphi$ is the volume element in oblate spheroidal coordinates.

Substituting (3) into (1) we obtain a system of ordinary differential equations [12]

$$\frac{d}{d\xi} (\xi^2 + 1) \frac{d}{d\xi} X_{mk} (\xi; R) - \left[\lambda - p^2 (\xi^2 + 1) - \frac{m^2}{\xi^2 + 1} \right] X_{mk} (\xi; R) = 0, \quad (5)$$

$$\frac{d}{d\eta} (1 - \eta^2) \frac{d}{d\eta} Y_{mq}(\eta; R) + \left[\tilde{\lambda} - p^2 (1 - \eta^2) - \frac{m^2}{1 - \eta^2} \right] Y_{mq}(\eta; R) = 0. \quad (6)$$

subject to boundary conditions $X_{mk}(0; R) = X_{mk}(\xi_0; R) = 0$ and $Y_{mq}(0; R) = Y_{mq}(\eta_0; R) = 0$. Here $p_j^2 = E_j R^2 / 2$ is the energy parameter, $\lambda = \lambda_{mk}^{(\xi)}(p)$ and $\tilde{\lambda} = \lambda_{mq}^{(\eta)}(p)$ are the separation constants. The energy spectrum is determined from the separation constant matching condition

$$\lambda_{mk}^{(\xi)}(p) = \lambda_{mq}^{(\eta)}(p). \quad (7)$$

Obviously, the spectrum scales as an inversed square of the characteristic ring size R .

3. Results

Consider a set of rings of a fixed volume V

$$V = \frac{\pi R^3}{4} \int_0^{\xi_0} \int_0^{\eta_0} (\xi^2 + \eta^2) d\xi d\eta = \frac{\pi R^3}{12} \xi_0 \eta_0 (\xi_0^2 + \eta_0^2). \quad (8)$$

Evidently, the parameters of the ring ξ_0 and η_0 enter this formula symmetrically. The ranges for ξ and η , however, and the corresponding coordinate surfaces are different (Figure 1). We can, thus, fix the volume and the characteristic radius of the ring in (8) and obtain a relationship between ξ_0 and η_0 $\xi_0 = f(\eta_0)$ which keeps the volume of the structure invariant. This way our approach allows us to study the influence of the ring shape on the structure of its spectrum.

The shape of the ring, however, is not managed by the parameter η_0 alone. Even though the spectrum of the model scales as the inversed square of the characteristic size of the ring $1/R^2$, this scaling breaks if we keep the volume of the ring fixed. So in order to make a comprehensive study of the ring shape effects, we should also vary the volume of the ring or its characteristic size. As the ring volume scales exactly as R^3 , it is just natural to introduce a dimensionless parameter $\sigma = V^{1/3}/R$ and use it as the second independent shape parameter.

We illustrate the variations of the ring shape for different values of shape parameters η_0 and σ in Figure 3. We can identify several distinctive cases. For smaller values of η_0 and bigger values of σ the ring surface is dominated by the hyperboloid inside the ring with nearly cylindrical section of the ellipsoid outside the ring. As η_0 approaches 1 for smaller σ we see the picture reversed: the major part of the boundary is formed by the ellipsoid outside with a nearly cylindrical section of the hyperboloid inside the ring. For bigger σ the ring looks like an ellipsoid with a hole. When the both shape parameters are small the ring looks like a one-dimensional structure. In Figure 4 we show the energy dependence $E_j(\eta_0)$ on the shape parameter η_0 for 12 lowest eigenstates of the ring. As $\eta_0 \rightarrow 0$ the ring is getting flat, and

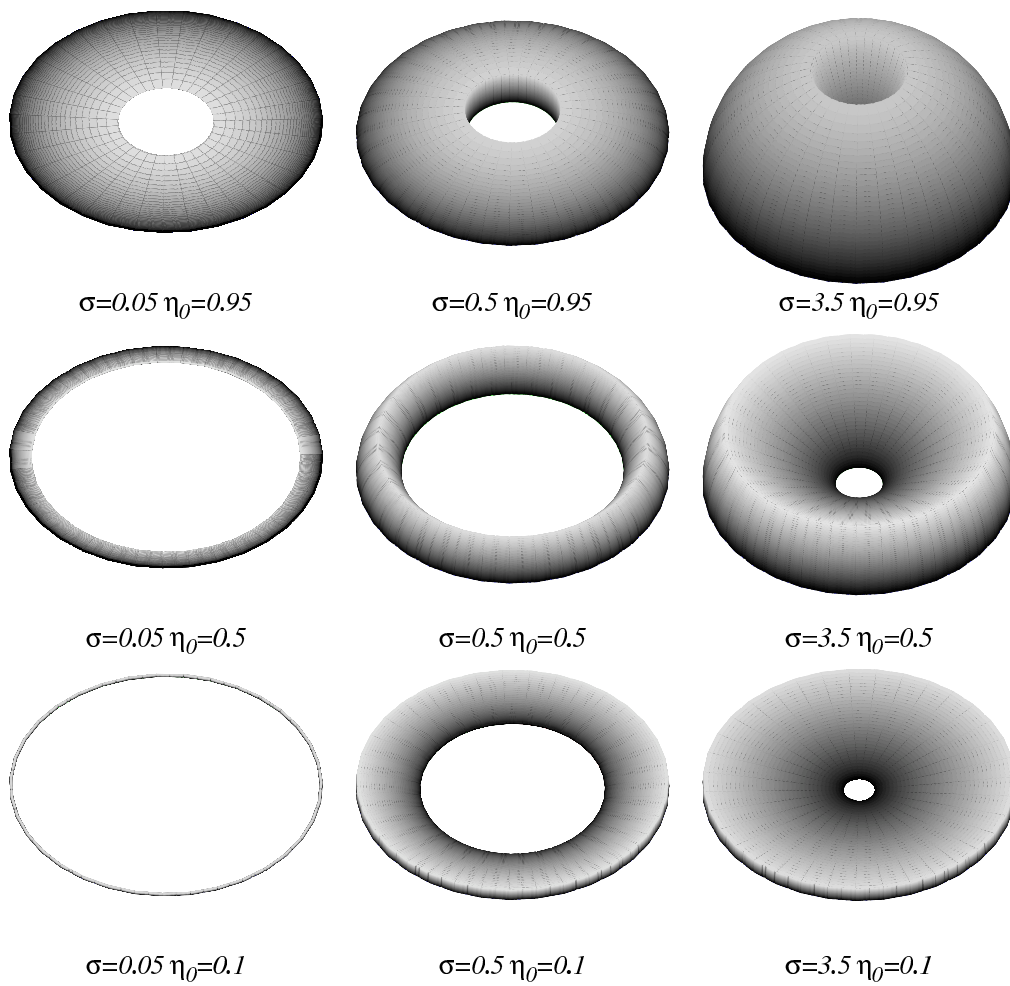


Figure 3: Ring shapes for different shape parameters η_0 and σ .

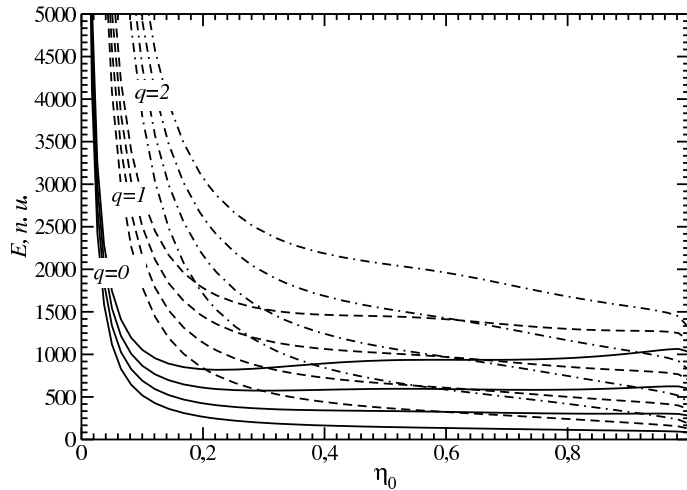


Figure 4: Energy dependence $E_{kq0} = E_{kq0}(\eta_0)$ on the shape parameter η_0 for the ground and the lowest 11 excited states for $\sigma = 0.5$, $R = 1$.

Table 1: Parametrization $\epsilon_{kqm} = \epsilon_{kq0} + \alpha_{kq} m^{\beta_{kq}}$ of the spectra for the rings of different shapes for $V = 1/2$ and $R = 1$.

kq	$\eta_0 = 0.1$	$\eta_0 = 0.5$	$\eta_0 = 0.95$
00	$200.9 + 0.16 m^{1.99}$	$47.9 + 0.66 m^{1.88}$	$26.1 + 2.46 m^{1.66}$
01	$700.8 + 0.14 m^{2.00}$	$127.8 + 0.50 m^{1.96}$	$56.7 + 3.33 m^{1.60}$
02	$1491.0 + 0.14 m^{2.00}$	$242.8 + 0.46 m^{1.97}$	$98.9 + 3.85 m^{1.59}$
10	$262.4 + 0.19 m^{1.99}$	$100.2 + 0.79 m^{1.88}$	$70.8 + 3.99 m^{1.58}$
20	$323.6 + 0.21 m^{1.97}$	$170.9 + 0.79 m^{1.91}$	$137.0 + 5.31 m^{1.54}$

the energy spectrum starts becoming degenerate in quantum number k as the corresponding degree of freedom contributes less and less to the total energy. It is also noteworthy that some of the curves $E_j(\eta_0)$ have minima. This newly discovered observation might have some implications for ring fabrication techniques.

Another, and, probably, more interesting example of the quantum ring spectrum shape dependence is the study of excitations in magnetic quantum number m . It is usually assumed that the spectrum of angular excitations in a quantum ring can be described by a simple one-dimensional model which predicts parabolic behavior of the excited states $E_m \propto m^2$ [19]. Our calculations, however, clearly demonstrate essential deviations from this rather common assumption.

Consider rings of different shapes as shown in Figure 3 at a fixed volume and calculate the lowest excitations E_{kqm} for $(kq) = (00), (01), (02), (10), (20)$ and $|m| = 0, 1, \dots, 30$. These energy levels are smooth functions of the quantum number

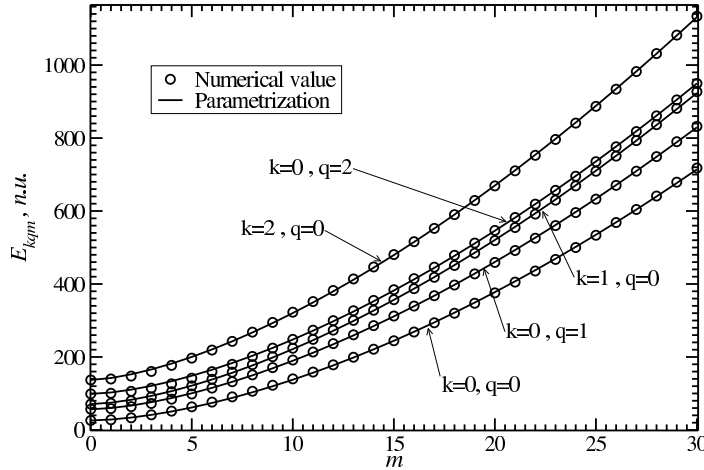


Figure 5: Quantum ring excitations and their fits for $V = 1/2$, $R = 1$ and $\eta_0 = 0.95$.

m , and their dependence on m is easy to fit with a simple parametrization $\epsilon_{kqm} = \epsilon_{kq0} + \alpha_{kq} m^{\beta_{kq}}$ as is shown in Figure 5. The one-dimensional ring model corresponds to $\beta_{kq} \equiv 2$, and the deviations of β from this value indicate that the quantum ring is essentially three-dimensional and should not be treated as a bended quantum wire. As an example, we present the parametrization of the quantum ring spectra for three different shape configurations in Table 1. In the case of a flat ring ($\eta_0 = 0.1$), we see that all the calculated states demonstrate the parabolic m dependence, and this ring configuration essentially follows the one-dimensional model. For the other two configurations, however, the value of β is measurably smaller than 2, and the one-dimensional model of the ring does not describe the energy spectrum of the "magnetic" excitations. In Figure 6 we show a contour map for the magnetic spectrum shape parameter β_{00} as a function of the ring shape parameters η_0 and σ . The maps for higher k and q have similar structure. The map demonstrates several interesting features.

First, there is a clear tendency for flat ring configurations ($\eta_0 < 0.125$) to produce m -dependence of the spectrum very close to the textbook m^2 behavior of 1D models. The configurations with more prominent 3D structure ($\eta_0 > 0.4$) generally produce spectra that deviate from the 1D model quite substantially.

Second, the configurations of small σ follow 1D-like dependence on the magnetic quantum number m for a broader range of configurations independent, basically, of the parameter η_0 . This is not surprising, as these configurations do look like as a 1D wire loop for smaller η_0 and become flat as η_0 increases.

Finally, there is a special set of shapes about $\sigma \approx 0.45$ and $\eta_0 > 0.95$ for which the deviation of the spectrum m -dependence from the 1D model is the most

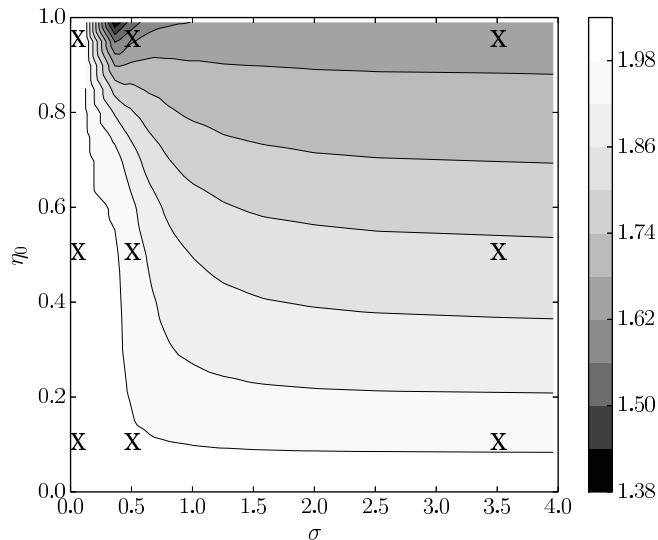


Figure 6: The magnetic quantum number excitation spectrum shape characteristic β_{00} for rings of different shapes. The marked points correspond to the ring configurations in Figure 3.

prominent. It is interesting to note that in the vicinity of this region we also see rapid change in the behavior of the spectrum from purely parabolic to non-parabolic while the variations of the ring shapes are rather small.

4. Conclusions

Even though oblate spheroidal coordinates are used rather rarely in quantum mechanical calculations, we see that their application to quantum rings is a natural choice which gives researchers flexibility in varying the structure geometry while securing computational efficiency. The use of oblate spheroidal coordinates for quantum ring calculations allowed us to discover a nontrivial shape dependence of the ring spectrum properties.

In this article we studied the model of a quantum ring formed in a potential well with infinite walls. We have shown that the corresponding Schrödinger equation admits separation of variables in oblate spheroidal coordinates. This allowed us to construct a classification of single-particle states in the quantum ring and to demonstrate essential dependence of the single-particle spectrum on the shape of the quantum ring. In particular, the most demonstrating example of such shape dependence can be seen by studying the dependence of the spectrum on the magnetic quantum number. We see, that a rather common assumption of parabolic dependence of 1D model should not be taken for granted, and quantum rings of many shapes that resemble realistic configurations are expected to demonstrate the spectra that scale as m^β with $1.3 < \beta < 2$.

We have performed our demonstration on the base of a simple boundary condition model. The first step towards more elaborated and realistic models would rely on the existence of potentials that admit separation of variables in oblate spheroidal coordinates while reproducing the interaction of a particle with the nano-structure of interest. Fortunately, the potentials that fit this description do exist and will be the subject of a separate publication.

Acknowledgements. Authors want to thank Prof. Slavyanov, Prof. Verbin, Prof. Abarenkov and Dr. Kovalenko for encouraging discussions.

References

- [1] Lorke A, Garcia J M, Blossey R, Luyken R J and Petroff P M, *Self-Organized InGaAs Quantum Rings—Fabrication and Spectroscopy*, Adv. Solid State Phys. 2003, **43**, pp.125–137
- [2] Somaschini C., Bietti S., Koguchi N. and Sanguinetti S., *Coupled Quantum Dot–Ring Structures by Droplet Epitaxy*, Nanotechnology 2011, **22**, 185602
- [3] Somaschini C., Bietti S., Sanguinetti S., Koguchi N., Fedorov A., Abbarchi M. and Gurioli M., *Fabrication of GaAs Concentric Multiple Quantum Rings by Droplet Epitaxy*, IOP Conf. Series: Materials Science and Engineering 2009, **6**, 012008
- [4] Wu J., Wang Z. M., Holmes K., Marega Jr. E., Zhou Z., Li H., Mazur Yu. I. and Salamo G. J., *Laterally Aligned Quantum Rings: from One-Dimensional Chains to Two-Dimensional Arrays*, Appl. Phys. Lett. 2012, **100**, 203117
- [5] Yabu H., *Bottom-Up Approach to Creating Three-Dimensional Nanoring Arrays Composed of Au Nanoparticles*, Langmuir 2013, **29**, pp.1005–1009
- [6] Li Y., Duan G. T., Liu G. Y. and Cai W. P., *Physical Processes-Aided Periodic Micro/Nanostructured Arrays by Colloidal Template Technique: Fabrication and Applications*, Chem. Soc. Rev. 2013, **42**, pp.3614–3627
- [7] Magarill L. I., Romanov D. A. and Chaplik A. V., *Electron Energy Spectrum and Continuous Current in the Elliptic Quantum Ring*, Zh. Eks. Teor. Fiz. 1996, **110**, pp.669–682 [JETP 1996, **83**, pp.361–367]
- [8] Ebrahim Heidari Semiromi, *The Aharonov–Bohm Oscillations and Energy Spectrum in Two-Dimensional Elliptical Quantum Ring Nanostructures*, Phis. Scr. 2012, **85**, 035706
- [9] Xiyang Ma and Caixin Lou, *Energy States of a Single Electron in a Three-Dimensional Quantum Ring*, Phis. Scr. 2010, **82**, 035704
- [10] Li Y., Voskoboynikov O. and Lee C. P., Tech. Proc. of the 2002 Inter. Conf. on Modeling and Simulation of Microsystems / Nanotech 2002, **1**, p.540

-
- [11] Filikhin I., Deyneka E., Melikyan H., Vlahovic B., *Electron States of Semiconductor Quantum Ring with Geometry and Size Variations*, Molecular Simulation 2005, **31**, pp. 779–785
- [12] Komarov I. V., Ponomarev L. I. and Slavyanov S. Yu., *Spheroidal and Coulomb Spheroidal Functions*. 1976, Moscow: Nauka [in Russian]
- [13] Morse P. M. and Feshbach H., *Methods of Theoretical Physics*. 1953, McGraw-Hill: New York
- [14] Rainwater J., *Nuclear Energy Level Argument for a Spheroidal Nuclear Model*, Phys. Rev. 1950, **79**, pp. 432–434
- [15] Gusev A. A., Chuluunbaatar O., Hai L. L., Vinitsky S. I., Kazaryan E. M., Sarkisyan H. A. and Derbov V. L., *Spectral and Optical Characteristics of Spheroidal Quantum Dots*, Journal of Physics: Conference Series 2012, **393**, 012011
- [16] Bin Li and Peeters F. M., *Tunable Optical Aharonov-Bohm Effect in a Semiconductor Quantum Ring*, Phys. Rev. B 2011, **83**, 115448
- [17] Abbarchi M., Mastrandrea C. A., Vinattieri A., Sanguinetti S., Mano T., Kuroda T., Koguchi N., Sakoda K. and Gurioli M., *Photon Antibunching in Double Quantum Ring Structures*, J. Phys. B 2009, **79**, 085308
- [18] Even J., Loualiche S., *Exact Analytical Solutions Describing Quantum Dot, Ring and Wire Wavefunctions* J. Phys. A: Math. Gen. 2004, **37**, pp. 289–294
- [19] Viefers S., Koskinen P., Singha Deo P., Manninen M., *Quantum Rings for Beginners: Energy Spectra and Persistent Currents*, Physica E 2004, **21**, pp. 1–35